Effect of Flow Reversal on the Shear Induced Formation of Multilamellar Vesicles

Florian Nettesheim,[†] Ulf Olsson,[‡] Peter Lindner,[§] and Walter Richtering*,[||]

Physical Chemistry, Christian-Albrechts-Universitat zu Kiel, Olshausen Strasse 40, D-24098 Kiel, Germany, Physical Chemistry 1, Lund University, Getingevegen 60, Box 124 SE-221 00 Lund, Sweden, LSS-Group, Institute Laue-Langevin, BP 156-38042 Grenoble Cedex 9, France, and Physical Chemistry, RWTH-Aachen, Templergraben 59, D-52056 Aachen, Germany

Received: October 22, 2003; In Final Form: January 14, 2004

The influence of rate controlled flow reversal on the transition from planar lamellae to multilamellar vesicles (MLV) using a nonionic lamellar phase consisting of 40 wt % triethylene glycol monodecyl ether ($C_{10}E_3$ in D_2O) is investigated by means of time-resolved rheo-small-angle light and neutron scattering (SALS, SANS). Flow reversal provides the possibility to control the kinetics of the transition substantially, and states occurring very early during the transition can be studied. A slowing down of the transition on an absolute strain axis is observed as the strain amplitude of the flow reversal is decreased. This retardation is attributed to the partial recovery of an earlier state as shear is inverted. This can nicely be demonstrated by the width of the azimuthal intensity distribution, which shows oscillations upon flow reversal. From the slowing down of the process a loss term is defined, which provides insight in the very early stages of the experiment, namely the minimum strain that is needed to induce irreversible structural changes in the sample. This quantity is for the present sample found to be 6.5 strain units. Furthermore, the exponential scaling of the strain needed to reach characteristic states of the transition with strain amplitude seems to hold for all length scales involved in the process.

Introduction

The influence of shear on lyotropic lamellar phases is of fundamental interest to industrial application as well as for mere scientific reasons. In particular, a control over the kinetics of multilamellar vesicle (MLV) formation would be useful. In view of their morphology they are interesting for applications as microreactors and for drug encapsulation.[1−3] The inherent nonequilibrium nature of MLVs poses problems for technological realization and understanding the time scales and specific conditions under which MLVs are formed is indispensable for a better control over the formation process.

It is well-known that multilamellar vesicles (MLV, also termed torical focal conic defects, spherulites, or onions) can be formed by shearing a lamellar phase.[4] Earlier studies focused on the steady-state behavior of the L_α phase. In this context so-called orientation diagrams were established, where areas of lamellar orientation in a shear field are mapped in a shear rate vs surfactant volume fraction diagram.[4] These orientation diagrams display a central region, where MLVs are present, neighbored by lamellae with parallel orientation. In certain regions of the orientation diagram transitions from planar lamellae in orientation parallel to perpendicular orientation and back have been observed as a function of shear rate.[4−7]

In the low shear region a defect ridden L_α phase is present. It has been proposed that such defects play a central role in MLV formation.[4] Leon et al.[8] describe the process of MLV formation as a randomly activated process.

Within the MLV region, the steady-state size of the MLVs is expected to scale with σ^{-1}.[11] This dependence is derived by balancing the surface tension of a droplet with bulk stress. Expressing the bulk stress by viscosity times shear rate and bearing in mind that the viscosity itself is shear rate dependent with a shear thinning exponent of $-1/2$, the proportionality of MLV size to $\dot{\gamma}^{-1/2}$, as often found in rate controlled experiments, can be rationalized.[4,9,10] However, a proportionality with $\sigma^{-0.75}$ was reported in the case of stress controlled experiments.[12] The evolution of the structure as displayed by physical properties, such as viscosity, conductivity, birefringence and the evolution of the scattering pattern, during the transition from planar lamellae to MLVs was found to scale with strain.[12−17]

Several different theoretical approaches have been proposed to model the mechanism of MLV formation. Zilman et al. proposed a coupling of strain with short wavelength thermal undulation, leading to a coherent stripe buckling of lamellae that will eventually lead to MLV formation.[18] The MLVs are expected to be of comparable size as the wavelength of the buckling instability. Further calculations about the influence of shear on lamellar systems were performed by Marlow and Olmsted.[19] They calculated how a lamellar phase escapes the tension induced by the suppression of thermal undulations by a shear field, predicting that impermeable bilayers have to buckle and eventually form closed bilayers (MLVs), whereas permeable lamellae have the possibility to reduce the lamellar spacing by creating new lamellae. For both proposed mechanisms a strain dependence of the process should be expected.

Courbin et al. found a $\dot{\gamma}^{1/3}$ dependence of the q vector, at which the intensity maximum of the first formed MLVs occurs, a strong evidence for the buckling mechanism proposed by Zilman et al.[15,16] Furthermore, they found the same scaling exponent for the dependence of the lamellar spacing d and the

* Corresponding author. E-mail: richtering@rwth-aachen.de. homepage: http://www.uni-kiel.de/phc/ags/richtering.
[†] Christian-Albrechts-Universitat zu Kiel.
[‡] Lund University.
[§] Institute Laue-Langevin.
[||] RWTH-Aachen.

10.1021/jp037189w CCC: $27.50
Published on Web 04/28/2004

inverse sample thickness $1/D$. The strain needed to induce the initial buckling, however, was only found to scale with the inverse of the lamellar spacing d.

Auernhammer et al.[20] proposed a hydrodynamic model based on the formalism of the description of thermotropic smectics, where the underlying nematic and smectic directors couple differently to the shear field.

Lyotropic lamellar phases and thermotropic smectic liquid crystals share most of the above-described features, except MLV formation. Large amplitude oscillatory shear (LAOS), however, has only been studied for thermotropic smectics, and it was found to drive out defects, if the strain amplitude was close to unity. Thus LAOS produces a defect free, oriented lamellar phase.[21]

Little is known about the effect of oscillatory shear on MLV formation itself. If lyotropic lamellar systems showed the same response to oscillatory shear as thermotropic smectics, namely the healing of focal conic defects, this would be an intriguing aspect.

Very recently an interesting study in this regard was pursued by Fritz et al.[22] They investigated the effect of an oscillating shear field on the formation kinetics of MLVs. Varying the stress amplitude of the oscillation, they were able to control the kinetics of the transition and to determine a minimum strain amplitude needed to trigger MLV formation. The steady-state size was, however, controlled by the stress amplitude, according to continuous shear experiments.[12] This study mainly relies on rheological information. The only structural information therein comes from rheo-SALS experiments, i.e., probing length scales of a few micrometers. Furthermore, the starting conditions are less well defined, because in the AOT−brine system, an orientation of the lamellae prior to shear is not possible. Consequently, the experiment was carried out with a polydomain sample.

Nonionic surfactant systems of the C_nE_m type have proved to be particularly useful for studying the transition from planar lamellae to MLVs under the influence of shear.[13,17] These systems are advantageous in two respects. On one hand they are binary systems, and therefore problems with different preferred curvature caused by a segregation of components, as is possible in ternary systems, are avoided; on the other hand, the bilayer saddle-splay modulus $\bar{\kappa}_b$ varies with temperature and thus offers a convenient way to study the transition as $\bar{\kappa}_b$ changes. Zipfel et al.[13] and Nettesheim et al.[17] studied the transition from planar lamellae to MLVs for continuous shear, varying shear rates, temperature, and surfactant chain length. The results from these studies will serve as references in the investigation presented here.

There are three major differences between the study of Fritz et al. and the one presented here. First, Fritz et al. use stress-controlled oscillatory experiments, whereas we use a zigzag strain profile (for details see section 3.1). Second, as pointed out above, Fritz et al. mainly rely on rheological information. We, however, will present structural information on two different length scales from small-angle neutron and small-angle light scattering experiments. Third, the initial state is in our case well-defined by preparing a lamellar phase in a parallel orientation, where the layer normal is parallel to the velocity gradient direction.

Experimental Section

The system contains the nonionic surfactant triethylene glycol monodecyl ether $C_{10}E_3$ (40 wt % in D_2O). A lamellar phase with predominant parallel orientation was prepared by continuously shearing the sample with $\dot{\gamma} = 10\ s^{-1}$ at 42 °C, as described previously.[13] SANS experiments were performed at the D11 beam line at the ILL in Grenoble, France. A thermostated Couette shear cell consisting of two concentric quartz cylinders with a gap of 1 mm was employed to study SANS under shear. The step motor enabled an easy inversion of the direction of shear by simply reversing the polarity. Two scattering configurations were used: The radial beam, where the neutrons pass along the gradient direction, and the tangential beam, where the neutrons pass along the flow direction. The sample was studied at $0.02\ Å^{-1} < q < 0.15\ Å^{-1}$. Data correction for background and solvent scattering, absolute calibration dividing as well as radial and azimuthal averaging was performed on the anisotropic data using Grasp, a standard ILL software. Radial averaging was performed in 30° sectors along the flow, neutral, and gradient directions whereas the azimuthal average was performed in a 360° sector at the Bragg peak position ($0.084\ Å^{-1} < q < 0.12\ Å^{-1}$).

Depolarized rheo-SALS experiments were performed using a Bohlin-CVO HR rheometer equipped with a quartz 3° cone/plate shear geometry. The incident light ($\lambda_0 = 488$ nm) was linearly polarized parallel to the flow direction and passed the sample along the gradient direction. The analyzer was aligned perpendicular to the polarization of the incident light. The accessible q-range in SALS was ca. $0.5-3\ \mu m^{-1}$. The evolution of the SALS patterns was captured by a CCD camera and saved in tiff format. For the evaluation of the depolarized scattering rheo-SALS patterns were selected in equal intervals along the strain axis.

Results

The presentation of the results will be divided into three sections. First, a description of the experimental protocol will be given. Second, we present the response of lamellar orientation as observed by SANS. Finally, the response on larger length scales will be discussed in connection to SALS data.

Procedures. Using a lamellar phase initially in the parallel orientation where the layer normal is parallel to the velocity gradient direction (for the preparation of this initial state see ref 13), flow reversal experiments were performed, employing shear rates of $\dot{\gamma} = 10$ and $5\ s^{-1}$ and varying strain amplitudes $\Delta\gamma$. Here, the strain amplitude is defined as $\Delta\gamma = \dot{\gamma}\Delta t$, with Δt the duration of half a shear cycle. This was accomplished by (1) shearing in one direction for a certain time at the given shear rate, yielding the desired strain, and then (2) shearing in the opposite direction for the same period of time and at the same shear rate.

Between (1) and (2) shear was stopped to give time for the recording of SANS spectra. The duration of the rest phase was chosen to yield scattering data with reasonable statistics. For the shear experiment itself, the duration of the rest phase is unimportant, because no structural changes take place, while shear is stopped.[17] Consequently, neutron scattering was only recorded at rest. This procedure was repeated until a total strain of $\gamma_a = 3 \times 10^4$ was reached. The resulting strain profile is as sketched in Figure 1.

To simplify comparison the same procedure was also used in rheo-SALS, except that scattering patterns were recorded during all phases of the experiment. Unless specified differently, the data (either SANS or SALS) are presented as a function of the absolute deformation $\gamma_a = \sum\gamma_{forward} + \sum\gamma_{backward}$, hence simply adding the values of the forward and backward shearing phases together. Figure 2 (left) displays a typical scattering pattern of an oriented lamellar phase recorded in the radial beam.

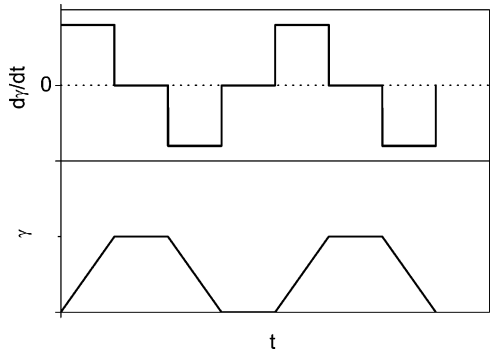

Figure 1. Profile of the flow reversal experiment.

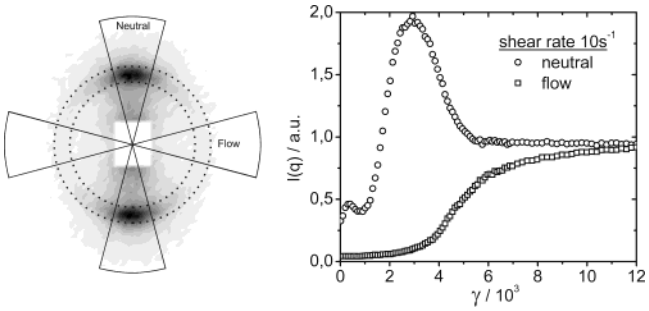

Figure 2. Left: neutron scattering of an aligned lamellar phase recorded in the radial beam. Solid lines are 30° radial sectors in neutral and flow directions, respectively. The dotted lines show the azimuthal sector at the Bragg peak position. Right: intensity trace along neutral and flow directions from a continuous shear experiment with $\dot{\gamma} = 10$ s^{-1} vs strain γ. The intensities are normalized to the intensity of the isotropic state. For two-dimensional SANS data of the continuous experiment see the Supporting Information or ref 17.

The sectors for radial and azimuthal averaging are depicted with solid and dotted lines, respectively.

The evolution of the scattering pattern during continuous shear was studied in previous experiments,[13,17] which now serve as a reference (Figure 2, right). To follow the progress of the transition with time or deformation, the intensity at the Bragg peak $I(q_0)$ was followed in the respective directions of the rheological experiment. This intensity evolution is termed an intensity trace.

Before the scattering in such a start-up experiment becomes isotropic due to MLV formation, the intensity in the neutral direction passes a maximum at $\gamma = 3000$, whereas the intensity in the flow direction is still very low. Tangential beam experiments at the same deformations revealed isotropic scattering symmetry. These two observations led to the conclusion that the anisotropy observed in the radial beam at $\gamma = 3000$ is indicative of the presence of a cylindrical symmetry in lamellar orientation.[13,17] This maximum in the neutral intensity trace will in the later experiments serve as the reference point for establishing reduced and relative strain axes.

Another point at much lower strain seems to be significant as well. A local maximum in the neutral intensity trace is observed at $\gamma \approx 300$. A temporary enhancement of the residual perpendicular orientation of lamellae causes this local maximum. The reproducibility of the starting point was checked in the tangential beam directly after preparing the oriented lamellar phase at 42 °C and at 25 °C just before starting the flow reversal experiment. Furthermore, the low viscosity of about 0.5 Pa s was indicative of a good parallel orientation of lamellae. The intensity found in the radial beam along the neutral direction prior to shear results from a small fraction of lamellae in the perpendicular orientation (where the layer normal is parallel to the vorticity direction). However, only about 10% of the lamellae reside in this orientation, which results in the initial anisotropy in the radial beam experiment.[13,17]

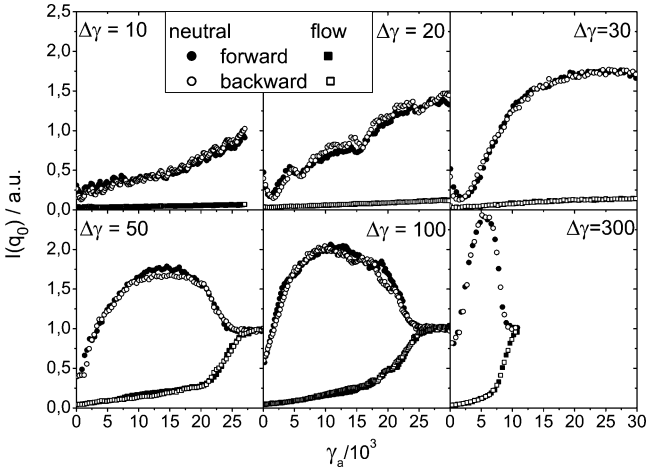

Figure 3. Intensity traces at q_0 along neutral and flow directions as a function of absolute strain for strain amplitudes 10, 20, 30, 50, 100, and 300 with shear rate 10 s^{-1}. The intensity traces of forward and backward shear are shown separately.

Small Length Scales. Using a shear rate of $\dot{\gamma} = 10$ s^{-1}, strain amplitudes $\Delta\gamma = 10$, 20, 30, 50, 100, 200, 300, 500, and 3000 were realized. Strain amplitudes 30 and 200 were studied in both beam configurations, the others only in the radial beam. The results of radial beam experiments are shown in Figure 3.

It can clearly be seen that the maximum of the neutral intensity trace, earlier identified with a cylindrical scattering symmetry,[13,17] shifts to higher absolute deformations as the strain amplitude of the flow reversal is decreased. At strain amplitudes below 30, passing the maximum was not accomplished within the course of the experiment. Here the position of the maximum was estimated by the intensity in neutral direction that was reached at the end of the experiment. This intensity was compared to that of a continuous experiment, and by extrapolation it was estimated how much more strain would be needed to reach the maximum in the neutral intensity trace assuming that the shape of the intensity traces is similar.

Nevertheless, contrary to what is typically found for the effect of large amplitude oscillatory shear on defect evolution in thermotropic smectic liquid crystals, MLVs (focal conic II defects) are still formed. Additionally, a broadening of the maximum in neutral direction with respect to absolute strain is found for decreasing $\Delta\gamma$ and the hight of the maximum decreases as well. The latter indicates that the intermediate structure is different; i.e., the buckling of the lamellae is less pronounced.

Interestingly, irregular oscillations of the intensity in the neutral direction with a period of 1300−5000 absolute strain units are observed for strain amplitudes 20 and 10, respectively. These oscillations become more regular with smaller $\Delta\gamma$. It can be assumed that these oscillations correspond to the first local maximum of the intensity trace in neutral direction at $\gamma = 300$, which was found in preceding experiments with continuous shear (compare Figure 2b). However, they are not observed at higher strain amplitudes. It is so far not understood why these oscillations disappear at higher strain amplitudes. Moreover, the absence of the first wiggle in the neutral intensity trace for $\Delta\gamma \geq 30$ remains unclear.

To study the influence of the shear rate, 5 s^{-1} was used, aiming for strain amplitudes of $\Delta\gamma = 30$ and 300, shown in Figure 4.

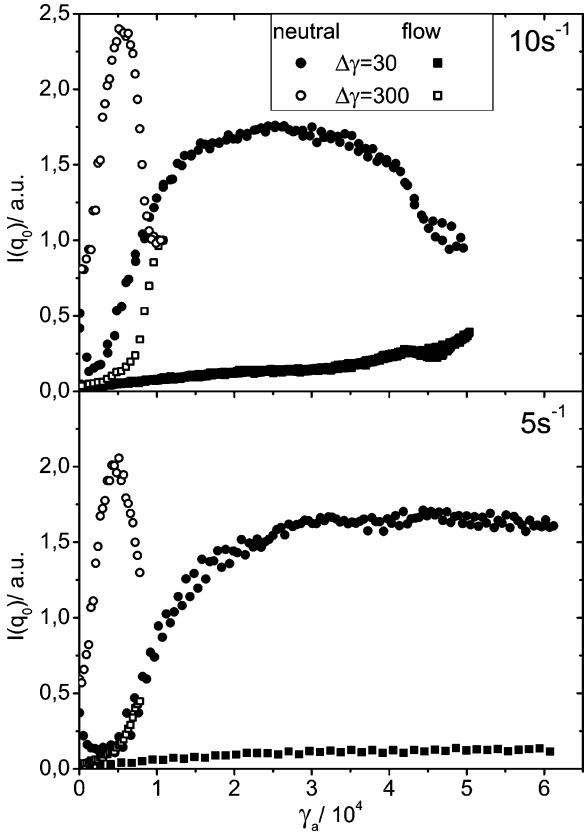

Figure 4. Intensity traces along neutral and flow directions as a function of absolute strain for strain amplitudes 30 and 300 with shear rates 10 s^{-1} (top) and 5 s^{-1} (bottom).

Qualitatively the same evolution of Bragg peak intensities is found as for the experiments conducted with 10 s^{-1}. The slowing down of the process with decreasing $\Delta\gamma$ is also observed. Even the absolute strain values at which the maximum of the neutral intensity trace is found, are quite similar. However, at $\Delta\gamma = 300$ the maximum is passed if 10 s^{-1} are applied, whereas the neutral intensity remains at a plateau value in the case of the 5 s^{-1} experiment.

So far the results of the flow reversal experiments display a certain loss of strain, as can be concluded from the shift of the intenisity maximum of the neutral trace to higher absolute strain values in comparison to a continuous experiment. Let us define a quantity similar to the loss factor of Fritz et al.[22] To quantify this loss, the maximum along the intensity trace in the neutral direction was taken as a reference point for establishing a master curve. This was accomplished by shifting the neutral intensity traces of the flow reversal experiments onto that of a continuous one. In every experimental cycle, a certain fraction of the strain contributes to MLV formation (irreversible dissipation) and, if shear is inverted a part of the strain that restores − at least partially − an earlier state. Thus, the resultant state with respect to a continuous experiment is given by

$$X = \frac{\gamma_{\max,\mathrm{cont}}}{\gamma_{\max}} \tag{1}$$

Here X is the fraction of strain that irreversibly contributes to MLV formation and $\gamma_{\max}$ and $\gamma_{\max,\mathrm{cont}}$ are the deformations at which the intensity maximum in neutral direction is found in a flow reversal and a continuous experiment, respectively. This quantity will be called a shift factor and it quantifies the irreversible part of the strain that in every experimental cycle contributes to MLV-formation.

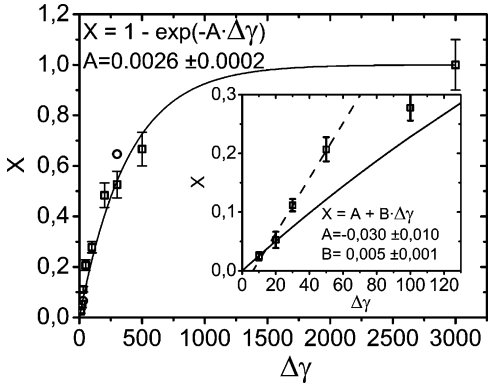

Figure 5. Shift factor X as defined in eq 1 as a function of strain amplitude for $\dot{\gamma} = 10^{-1}$ (squares) and 5^{-1} (circles). The solid line represents a best fit to the data using $X = 1 - \exp(-A\Delta\gamma)$ as a test function. The inset shows $\Delta\gamma < 130$ for which a linear fit was chosen (dashed line). For comparison $X = 1 - \exp(-A\Delta\gamma)$ is included (solid line).

It has to be mentioned that X is only representative for one point in the course of the whole experiment, i.e., the occurrence of the maximum anisotropy in the neutral intensity trace. This will also become evident at a later point of the discussion. Nevertheless it is a feasible criterion for determining the progress of and the average reversible and dissipative contributions to the transition. The result of this calculation is presented in Figure 5.

In this representation $X = 0$ means that the reversible part of the strain dominates and hence there will be no transition from planar lamellae to MLVs. As can be seen from this representation of the data, the slowing down of the transition can be described by an exponential function of the form $X = 1 - \exp(-A\Delta\gamma)$ over the whole strain range. Taking a closer look reveals that the data at low strain amplitudes are not well represented by the overall scaling with $1 - \exp(-A\Delta\gamma)$. Yet a determination of a minimum strain amplitude $\Delta\gamma_{\min}$, below which a transition would not take place is difficult owing to the large error bars. The exponential scaling would for all finite values of $\Delta\gamma$ lead to positive values for the loss factor. The inset in Figure 5 displays a linear fit to the shift factor X for $\Delta\gamma < 50$ and consistently $\Delta\gamma_{\min}$ is found to be ≈6.5 strain units. However, this fit only describes the lowest strain amplitudes better and deviates substantially at higher values. We can thus conclude here that the minimum strain amplitude $\Delta\gamma_{\min}$ is to be found in the range of $0 \leq \Delta\gamma_{\min} \leq 6.5$.

Although only 2 points are available for the experiment with 5 s^{-1}, the slope is steeper and hence $\Delta\gamma_{\min}$ larger. The transition at 5 s^{-1} from planar lamellae to MLVs, as studied in a continuous experiment,[17] does not yield the final state of densely packed, but that of polydisperse MLVs. Thus it seems plausible that also the minimum strain required for MLV formation is larger.

However, the representation of the data in Figure 5 does not give information about the whole transition. Therefore the intensity trace along the neutral direction of the different experiments is plotted vs the absolute deformation γ_a normalized to the position of the respective maxima along the absolute strain axis, i.e., $\gamma_{\max}$. For a better comparison the intensity is normalized to 1 (Figure 6).

It can clearly be seen that the traces of the flow reversal experiments do not superimpose over the entire experiment. Before the intensity maximum the traces of the flow reversal

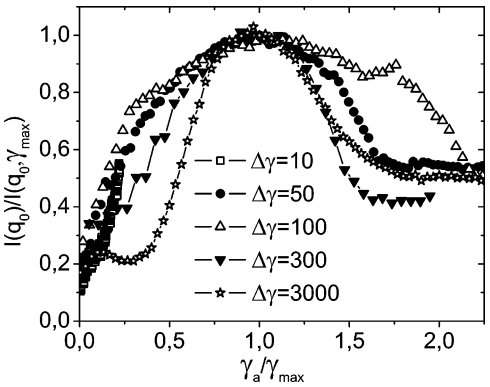

Figure 6. Neutral intensity traces for different strain amplitudes at $\dot{\gamma} = 10\ s^{-1}$ normalized to one vs absolute strain normalized to γ_{max}.

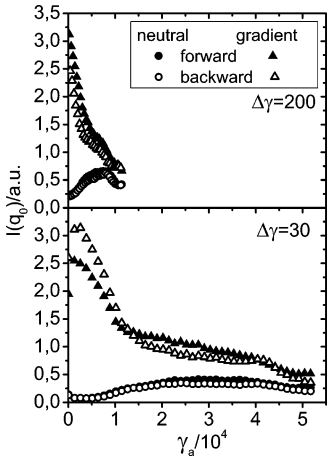

Figure 7. Intensity traces along neutral and gradient directions from tangential beam experiments for strain amplitudes 30 and 200, $\dot{\gamma} = 10\ s^{-1}$.

experiment display an immediate increase on the normalized strain axis, contrary to the trace of the continuous experiment. As was proposed by Zipfel et al., the transition involves two steps, the formation of cylindrical intermediates, multilamellar cylinders or coherently buckled lamellae. Consequently, the situation after the maximum, i.e., for $\gamma_a/\gamma_{max} \geq 1$, differs from that for $\gamma_a/\gamma_{max} \leq 1$. The fact that the traces do not superimpose over the entire strain range for $\gamma_a/\gamma_{max} \leq 1$ is not unexpected and is congruent with the observations made in the tangential beam experiment, as will be discussed in the section below.

Envisioning the transition from planar lamellae to MLVs as a process of successive lamellar fission, reorientation, and fusion, one can assume that the observed oscillation in the intensity trace of the neutral direction is due to slight reorientation processes of lamellae. These reorientations seem to be partially reversible. The irreversible part contributes in each cycle to the formation of MLVs.

This was further investigated in a tangential beam experiment using $\Delta\gamma = 30$ and 200. Because this beam configuration is especially sensitive to the parallel orientation of lamellae, one could expect distinct influences of the lamellar reorientation on the intensity distribution (Figure 7).

Qualitatively, the traces of the intensities in gradient and neutral directions are similar to those of a continuous experiment, only that it takes much larger absolute strain. The data recorded after shearing forward (closed symbols) or backward (open symbols) are shown separately. It is evident that up to absolute deformations of about 1×10^4 shearing backward leads to a partial recovery of Bragg peak intensity in the gradient

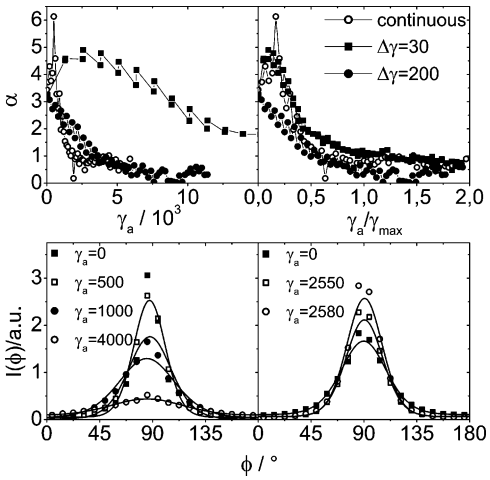

Figure 8. Top left: α as a function of absolute strain for strain amplitudes $\Delta\gamma = 30$, 200 and a continuous experiment, $\dot{\gamma} = 10\ s^{-1}$. A higher α implies a better alignment of the lamellae. Top right: scaling of the three respective experiments on a normalized strain axis. Bottom: Azimuthal intensity distributions including fits according to Piken et al. for a continuous (left) and a flow reversal experiment with $\Delta\gamma = 30$ (right).[25]

direction. In the course of the experiment the forward and backward shearing result in increasingly similar lamellar orientations.

For a better quantification of this observation the angular intensity distributions (Figure 8, bottom) were fitted to a model, because then the information of the whole azimuthal intensity distribution is taken into account, and not only the peak intensities. For this purpose a Mayer−Saupe description for the azimuthal intensity distributions of rodlike scatterers, as proposed by Piken et al., was employed.[23]

$$I(q_0,\phi) = I_0 \exp[\alpha P_2(\sin\phi)] + I_b \qquad (2)$$

Here I_0 and I_b are intensity amplitude and isotropic scattering contribution, respectively, and P_2 is the second Legendre polynomial. A phase of $\pi/2$ was subtracted from the orientation angle ϕ to account for the parallel alignment of lamellae. Additionally, α is proportional to the probability of finding a parallel lamellar orientation and thus accounts for the width of the angular intensity distribution. More details about this and other models for the calculation of the azimuthal intensity distribution of anisotropic scatterers can be found in ref 24. Figure 8 (top, left) displays the evolution of α for tangential beam experiments of continuous and flow reversal experiments calculated up to absolute strains of 1.5×10^4. As expected, α decreases with increasing absolute strain in the course of MLV formation until it reaches a steady-state value. In the experiment with $\Delta\gamma = 30$ and in the continuous one an ordering is observed in the beginning ($\gamma_a \leq 1000$); i.e., α displays a maximum at $\gamma_a \approx 3000$. In both flow reversal experiments α oscillates as long as the steady state is not reached and the amplitude of this zigzag is of comparable magnitude. For comparison, the evolution of α of the corresponding continuous experiment is supplemented.

In the shear experiment with $\Delta\gamma = 200$ scattering was recorded every cycle after both the forward and backward shear, whereas for $\Delta\gamma = 30$ only every 20 cycles after both forward and backward shear periods. The more astonishing is the fact that the oscillations in the latter case are still so prominent and regular.

Figure 8(top, right) shows the scaling of the three experiments on a strain axis normalized to the respective strains at which the maximum of the neutral intensity trace from a radial beam

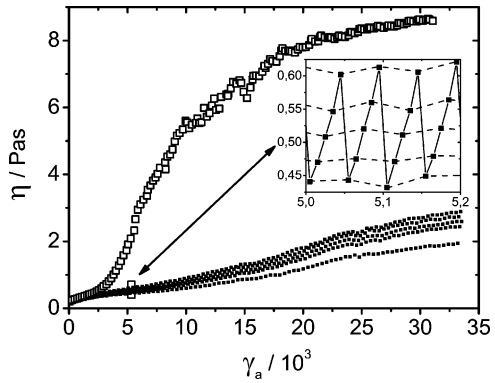

Figure 9. Transient viscosities of a flow reversal experiment with $\Delta\gamma = 50$ (closed squares) compared to a continuous one (open squares), both conducted with $\dot{\gamma} = 10\ s^{-1}$. The inset shows a zoom of the flow reversal experiment into the region just above $\gamma_a = 5 \times 10^3$.

experiment occurs. Again, it becomes evident that the strict scaling with $1 - \exp(-A\Delta\gamma)$ does not apply over the entire strain range. Nonetheless, the experiments show parallel behavior, as for instance steady state is reached at $\gamma_a/\gamma_{max} \approx 0.5$, just about where the oscillations of α in the flow reversal experiments damp. Figure 8(bottom) shows the fits of the intensity distributions according to Piken et al. for a continuous experiment (left) and the flow reversal experiment (right) with $\Delta\gamma = 30$, both using $\dot{\gamma} = 10\ s^{-1}$. The fits show a good agreement with the data and the widening of the intensity distributions proceeds symmetrically around 90°; i.e., the distribution of lamellar orientations is symmetric throughout the entire transition. Hence, the material transport in gradient direction that has to occur to bend or reorient lamellae, is symmetric as well. Clockwise flow in the neutral-gradient plane would lead to an asymmetry of the intensity distribution and, consequently, is compensated by a counterclockwise flow. Admittedly, the azimuthal intensity distributions are affected by the asymmetry of the tangential beam and thus systematic errors are introduced, impeding a more detailed discussion of this observation.

Large Length Scales. Rheo-SALS experiments were performed with a strain amplitude of $\Delta\gamma = 50$ and a shear rate of $\dot{\gamma} = 10\ s^{-1}$. The transient viscosities of this experiment are compared with those of a continuous one up to an absolute strain of $\gamma_a = 3 \times 10^4$ in Figure 9.

Most striking are the much lower viscosities during the entire experiment. The final viscosity is by a factor of ca. 3 smaller. Furthermore, the display of five distinct branches is somewhat peculiar. A closer look (inset in Figure 9) reveals that these are not separate branches, but a saw-tooth pattern of the viscosity evolution. Each upward trend of the viscosity, comprising five points, corresponds to a forward or backward shearing phase, respectively. Hence, inverting the direction of shear first decreases the viscosity, and then it increases again. Overall, this results in a net increase of the viscosity. It has to be mentioned that the decrease in the viscosity is not due to a relaxation of the structure upon cessation of flow. This was studied in earlier experiments, where step-strain experiments were performed, recording SANS patterns during the phases of rest.[17] The decrease in viscosity observed here are therefore merely due to the flow reversal.

These observations indicate that the process of MLV formation in a flow reversal experiment is not only slowed, but the mesoscopic structures at the end of the flow reversal experiment most likely differ substantially in comparison to the continuous experiment. The terminal viscosity of the flow reversal experiment is equivalent to the transient viscosity of the continuous experiment at strain values of ca. 6000. This would result, in analogy to the treatment of the neutron scattering data, in a shift factor $X = 0.18$. Recall, the value for $\Delta\gamma = 50$ calculated from the SANS experiments is 0.21 and the fit to the data yielded ca. 0.12.

The depolarized SALS patterns of the flow reversal experiment are arranged in Figure 10. Scattering patterns for deformations larger than 13 500 were not available in the flow reversal experiment, because gradual sample loss impeded recording meaningful data.

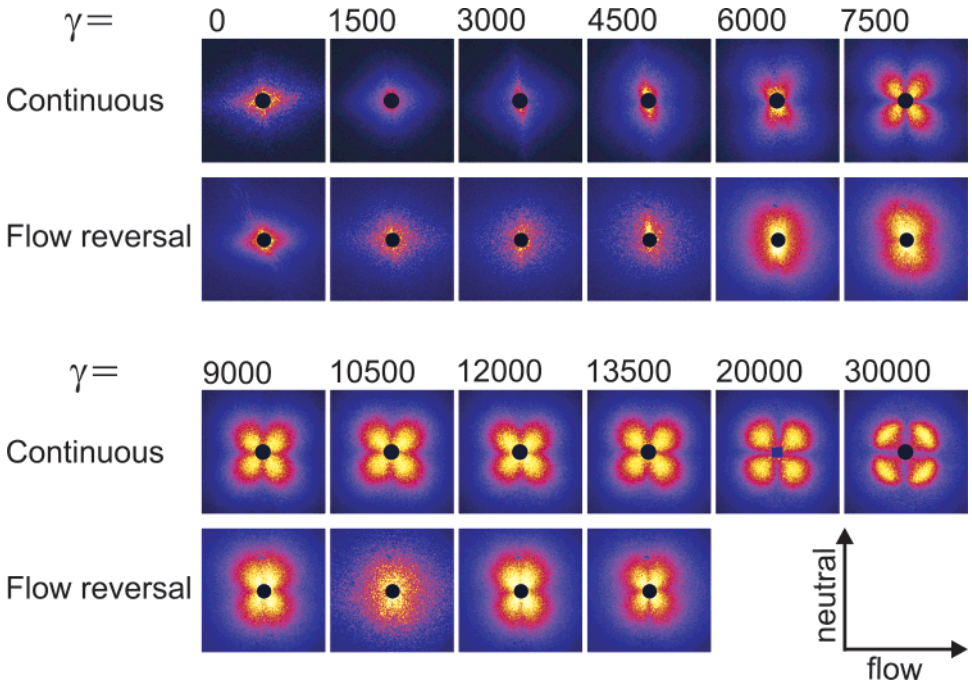

Figure 10. Depolarized SALS patterns recorded during the flow reversal experiment with a strain amplitude of $\Delta\gamma = 50$ at different absolute strain values compared to the scattering found during a continuous shear experiment with a shear rate of $10\ s^{-1}$ at the respective deformations.

As a function of absolute strain the scattering symmetry changes from two- to 4-fold at about 5500 absolute strain units. However, the cloverleaf pattern is elongated in neutral direction, thus indicating that the MLVs are elongated in flow direction. In these stages of the experiment, the 4-fold symmetry can disappear again as shear is inverted. At higher deformation the 4-fold symmetry is maintained; however, the orientation can vary slightly. The MLVs are still slightly elongated along the flow direction and the size of the aggregates can be estimated from the position of the intensity maximum with $R = 4.1/q_{max}$[26,27] to ca. 8 μm. The steady-state structure of the continuous experiment at a shear rate of $\dot{\gamma} = 10\ s^{-1}$, on the other hand, is a densely packed MLV phase, displaying a structure factor in depolarized SALS, from which a MLV size of 2.6 μm can be deduced.

Thus findings in the flow reversal differ fundamentally from those in the continuous experiments. First the size of the MLVs is much larger (about 3-fold, comparable to the decrease in viscosity) and about what is found at strain values of 6000 in a continuous experiment.

The cloverleaf displays an elongation in both cases, indicating elliptically deformed MLVs with an aspect ratio of about 1.5. Additionally, the intermediate vanishing and reoccurring of the 4-fold symmetry is unique to flow reversal.

Discussion

Flow reversal has a profound influence on the transition from planar lamellae to MLVs. The most obvious is the slowing down of the process. The neutron scattering data were compared to those of a continuous shear experiment with the respective shear rate, and an exponential scaling of the shift factor X with the strain amplitude $\Delta\gamma$ was observed. This scaling was found to hold for other length scales as well; namely, it was possible to relate the terminal viscosity of the flow reversal experiment with $\Delta\gamma = 50$ to the transient viscosity of a continuous experiment.

Also the data from depolarized SALS show a retardation of the process comparable to that observed by SANS and rheology. First evidence of MLVs is, however, already found at absolute strain values of ≈6000, comparable to the continuous experiment. The MLVs formed in this phase of the experiment can vanish again or deform in such a way that their scattering loses its 4-fold symmetry. This observation was also made by Fritz et al.[22] Presumably, the MLVs are stretched in the flow direction such that the characteristic cloverleaf pattern is not resolved by the SALS setup anymore.

The experiments in SANS and rheo-SALS give information about different length scales that are relevant for the process. Using these techniques, it should be possible to unravel the origin of the scaling of X with $1 - \exp(-A\Delta\gamma)$.

Shearing a lamellar phase leads to a structural change, which above certain deformations is irreversible. At deformation amplitudes of 3000 an inversion of shear direction did not have a noticeable influence on the process; flow reversal with $\Delta\gamma = 500$ already led to a slowing down of the process. At all strain amplitudes below 3000 there has to be a reversible and an irreversible component, the latter contributing to the formation of MLVs in each experimental cycle. At $\Delta\gamma = 3000$ the irreversible part is assumed to dominate completely.

To shed more light on this observation, we would like to compare these results with those obtained by Fritz et al. Their definition of the absolute strain is very similar to our's, although they applied oscillatory stress rather than a zigzag strain profile at a given shear rate. They calculate the loss factor by shifting the complex viscosity of an oscillatory onto that of a creep experiment, i.e., using rheological information to establish a mastercurve. This is different from our approach, where structural information from SANS experiments is used to establish a relative strain axis. The shift or loss factor, obtained by either of these methods, is not identical to the loss modulus G'', because it only gives information about the strain that leads to dissipation contributing to MLV formation. There are, however, other dissipation modes such as solvent viscosity that contribute to the loss modulus.[22]

The minimum deformation amplitude for shear rate 10 s^{-1} necessary to induce the transition from planar lamellae to MLVs ($\Delta\gamma_{min}$) is in our study found to be ≈6.5. This is of comparable magnitude to the value found by Fritz et al. for the AOT/Brine system. However, the use of different experimental procedures and even more the use of different surfactant systems, forbids a direct comparison. The AOT/Brine system used by Fritz et al. is a screened ionic lamellar phase, essentially representing a Helfrich stabilized system, as is also the case for the nonionic surfactant lamellar phase used in our study. However, the lamellar spacing is more than 2 times larger than in the $C_{10}E_3$/D_2O system studied here (≈135 and 60 Å, respectively).

The order parameter analysis of the tangential beam data revealed periodic changes of the width of the azimuthal intensity distributions with the absolute strain. This, to our knowledge, is a new aspect. These oscillations can be explained by changes of the lamellar order, e.g., building up coherent buckling of the lamellae. Upon flow reversal a previous state is at least partially restored and thus a lamellar phase with a higher degree of order is recovered. We speculate that only the part of the process that involves braking lamellae while changing its orientation is irreversible and consequently leads to MLV formation.

For larger length scales, i.e., rheo-SALS, indicating that $\Delta\gamma_{min}$ is independent of length scales. The question of the influence of shear rate is, however, still unresolved, although the experiments with 5 s^{-1}, as expected, indicate a slightly larger $\Delta\gamma_{min}$ (Figure 5).

The minimum strain needed to induce irreversible changes in the sample is much smaller in the beginning and accordingly increases in the course of the experiment. This conclusion is nicely supported by the oscillations in the lamellar orientation distribution α in the beginning of the experiment, which vanish before γ_{max} is reached. It is also the reason that even at the smallest strain amplitudes used in the experiment a transition takes place.

Conclusion

In the study presented here it was possible to show the effect of successive flow reversals on the transition from planar lamellae to MLVs. A slowing down of the process was observed, which scaled with $1 - \exp(-A\Delta\gamma)$. From establishing master curves we were able to distinguish a reversible from an irreversible contribution to the transition.

Tangential beam experiments and the order parameter analysis revealed that the change of the lamellar orientation distribution is partially reversible. A strong indication for such a process, namely, partially reversible reorientations of lamellae, are the oscillations observed early during the transition from planar lamellae to MLVs in the order parameter. The part of the process that involves breaking lamellae and not just bending them might represent the irreversible contribution to the transition.

A minimum strain required to induce irreversible changes in the sample was deduced from the irreversible contribution to the transition, yielding $0 \leq \gamma_{min} \leq 6.5$ strain units, comparable to the value found by Fritz et al. in stress controlled oscillatory experiments with an AOT/brine system. However, the systems

and experimental techniques used are too different to draw any conclusions from a comparison of the two studies. We, however, for a given low shear rate, here 10 s^{-1}, expect a minimum strain amplitude from the fact that the lamellar phase is a viscoelastic liquid at small enough strain amplitudes, i.e., in the linear viscoelastic regime. This value, in fact, can be very small.

An investigation of the dependence of γ_{min} on the lamellar spacing was not the scope of this study but could be subject to future work. This would be of particular interest with respect to the studies of Courbin et al.

Current theories describe the formation of MLVs from planar lamellae with parameters such as the strain or the strain rate. These descriptions are able to predict the strain control[18] that is also found experimentally or give estimates of a critical shear rate required for MLV− formation.[20] Both approaches also yield estimates of the initial size of the MLVs. The experimental data gathered here are not discussed in terms of current theories, because the influences of the various parameters (strain, shear rate, and stress) seem not to be independent of one another. A verification or falsification of the theories is not possible, because they apparently do not capture the interdependency of the variable parameters. We are confident that the data presented here will be useful to refine the current theoretical descriptions of this transition.

Acknowledgment. We thank the Deutsche Forschungsgemeinschaft (DFG), the Fond der Chemischen Industrie, and the Swedish Research Council for financial support.

Supporting Information Available: Two-dimensional SANS patterns in the radial and the tangential beam of $C_{10}E_3$ (40 wt % in D_2O) at three different strain values in a continuous shear experiment with a shear rate of 10 s^{-1}. This material is available free of charge via the Internet at http://pubs.acs.org.

References and Notes

(1) Gauffre, F.; Roux, D. *Langmuir* **1999**, *15*, 3738.
(2) Colin, A.; Roux, D. *Eur. Phys. J. E.* **2002**, *8*, 499.
(3) Bernheim-Grosswasser, A.; Ugazio, S.; Gauffre, F.; Viratelle, O.; Mahy, P.; Roux, D. *J. Chem. Phys.* **2000**, *112*, 3424.
(4) Roux, D.; Nallet, F.; Diat, O. *Europhys. Lett.* **1993**, *24*, 53.
(5) Zipfel, J.; Berghausen, J.; Lindner, P.; Richtering, W. *Europhys. Lett.* **1998**, *43*, 683.
(6) Berghausen, J.; Zipfel, J.; Diat, O.; Naranayan, J.; Richtering, W. *Phys. Chem. Chem. Phys.* **2000**, *2*, 2623.
(7) Zipfel, J.; Berghausen, J.; Lindner, P.; Richtering, W. *J. Phys. Chem. B* **1999**, *103*, 2841.
(8) Leon, A.; Bonn, D.; Meunier, J. *Phys. Rev. Lett.* **2000**, *84*, 1335.
(9) Müller, S.; Börschig, C.; Gronski, W.; Schmidt, C.; Roux, D. *Langmuir* **1999**, *15*, 7558.
(10) Panizza, P.; Colin, A.; Coulon, C.; Roux, D. *Eur. Phys. J. B* **1998**, *4*, 65.
(11) van der Linden, E.; Hogervorst, W. T.; Lekkerkerker, H. N. W. *Langmuir* **1996**, *12*, 3127.
(12) Bergenholtz, J.; Wagner, N. J. *Langmuir* **1996**, *12*, 3122.
(13) Zipfel, J.; Nettesheim, F.; Lindner, P.; Le, T. D.; Olsson, U.; Richtering, W. *Europhys. Lett.* **2001**, *53*, 335.
(14) Escalante, J. I.; Gradzielski, M.; Hoffmann, H.; Mortensen, K. *Langmuir* **2000**, *16*, 8653.
(15) Courbin, L.; Pon, R.; Rouch, J.; Panizza, P. *Europhys. Lett.* **2003**, *61*, 275.
(16) Courbin, L.; Delville, J. P.; Rouch, J.; Panizza, P. *Phys. Rev. Lett.* **2002**, *89*, 148305.
(17) Nettesheim, F.; Zipfel, J.; Olsson, U.; Renth, F.; Lindner, P.; Richtering, W. *Langmuir* **2003**, *19*, 3603.
(18) Zilman, A. G.; Granek, R. *Eur. Phys. J. B* **1999**, *11*, 593.
(19) Marlow, S. W.; Olmsted, P. D. *Eur. Phys. J. E* **2002**, *8*, 485.
(20) Auernhammer, G. K.; Brand, H. R.; Pleiner, H. *Phys. Rev. E* **2002**, *66*, 1707.
(21) Horn, R. G.; Kleman, M. *Ann. Phys.* **1978**, *3*, 229.
(22) Fritz, G.; Wagner, N. J.; Kaler, E. W. *Langmuir* **2003**, *19*, 8709.
(23) Piken, S. J.; Aerts, J.; Visser, R.; Northolt, M. G. *Macromolecules* **1990**, *23*, 3849.
(24) Hoekstra, H.; Vermant, J.; Mewis, J.; Naranayan, T. *Langmuir* **2002**, *18*, 5695.
(25) A small difference of the intensities prior to the shear experiment (bottom plots) arises from the positioning of the tangential beam. The two measurements, i.e., continuous and flow reversal, were performed during different beam times, and thus it is likely that the position at which the neutrons pass through the gap is not identical.
(26) Stein, R. S.; Wilkes, G. L. In *Structure and Properties of Oriented Polymers*; Ward, I. M., Ed.; Applied Science: Braking, Essex, U.K., 1975.
(27) Läuger, J.; Weigel, R.; Berger, K.; Hiltrop, K.; Richtering, W. *J. Colloid Interface Sci.* **1996**, *181*, 521.